DEUTSCHES ELEKTRONEN-SYNCHROTRON **DESY**

DESY 85-099
September 1985

RENORMALIZATION SCHEME DEPENDENCE OF ELECTROWEAK RADIATIVE CORRECTIONS

by

W. Hollik, H.-J. Timme

II. Institut f. Theoretische Physik, Universität Hamburg

ISSN 0418-9833

NOTKESTRASSE 85 · 2 HAMBURG 52

To be sure that your preprints are promptly included in the
HIGH ENERGY PHYSICS INDEX ,
send them to the following address (if possible by air mail) :

DESY
Bibliothek
Notkestrasse 85
2 Hamburg 52
Germany

DESY 85-099
September 1985

ISSN 0418-9833

Renormalization Scheme Dependence of Electroweak Radiative Corrections

W. Hollik and H.-J. Timme

II. Institut für Theoretische Physik der Universität Hamburg
D-2000 Hamburg, Federal Republic of Germany

Abstract: We compare two renormalization schemes of the electroweak standard model: the on-shell scheme with e, M_W, M_Z, M_H, and the fermion masses $\{m_f\}$ as free parameters, and an intermediate scheme where the W boson self energy is renormalized at $q^2 = 0$ instead of $q^2 = M_W^2$. Using the same physical input data for both schemes, various Green functions, the $M_W - M_Z$ mass relation, and the differential $e^+e^- \to \mu^+\mu^-$ cross section are calculated in one-loop order. We find striking differences between the forward-backward asymmetries predicted in either of the schemes near the Z resonance.

1. Introduction

Predictions of the electroweak standard modell [**1**] have been confirmed by the discovery of the W and Z bosons with the expected masses [**2**]. The next step of precision tests of the standard model beyond the tree level requires theoretical predictions which are normally based on perturbative calculations of radiative corrections. The renormalizability of the model [**3**] ensures that this is possible by multiplicative renormalization. Radiative corrections have been calculated to one-loop order for various processes: low energy processes (μ lifetime, ν scattering) [**4,5,6,7,8,9**] and high energy e^+e^- annihilation [**10,11**]. For calculations beyond the tree level it is necessary to specify a renormalization scheme, which defines

- the free parameters in the Lagrangian,
- the renormalization conditions in order to express the bare parameters and fields in terms of the renormalized ones,
- the connection of the free parameters with the experimental input data.

One can distinguish between three types of renormalization schemes applied in electroweak loop calculations:

(i) The on-shell scheme [**4,5,6,12**] makes use of the masses M_W, M_Z, M_H, $\{m_f\}$ of the massive vector bosons, the scalar Higgs boson, and fermions as free parameters. The renormalization conditions fix the finite parts of the renormalization constants in a way that directly allows for the particle content of the theory. Besides the masses, $e = \sqrt{4\pi\alpha}$ (α being the electromagnetic fine-structure constant) is commonly used as a precisely measured coupling constant.

(ii) Instead of the gauge boson masses M_W and M_Z, the renormalization can be based on the use of low energy parameters G_F and θ_W, where G_F is the μ decay constant and θ_W the weak mixing angle measured e.g. in $\nu_\mu e/\bar{\nu}_\mu e$ scattering [**7,8**]. The renormalization conditions ensure that G_F^2 determines the μ lifetime τ_μ and $\sin^2\theta_W$ the contribution of electromagnetic current to the weak neutral current. M_W and M_Z then can be derived by determination of the poles of the corresponding renormalized propagators.

(iii) The $\overline{MS}$ scheme [**9**] has the advantage that all the renormalization constants are fixed by the simple prescription of subtracting the singular parts of the two- and three-point functions. However, after relating the parameters $\alpha(\mu)$, $m_W(\mu)$, $m_Z(\mu)$, $m_H(\mu)$, and $\{m_f(\mu)\}$ to the corresponding physical quantities, this scheme becomes as complicated as (i) and (ii) [**13**].

For a survey see [14].

Due to the renormalization group invariance all renormalization schemes are equivalent. However, as long as we can only approximate physical observables by perturbative calculations these approximations are renormalization scheme dependent: the results in a fixed order given in different schemes deviate from each other by higher order contributions. This, however, does not mean a quantitative numerical estimate. Consequently, for testing the reliability of electroweak one-loop calculations, different renormalization schemes have to be compared with respect to their numerical predictions for measurable quantities.

The intention of this paper is to investigate the size of the renormalization scheme effect in the calculation of one-loop corrections to the following observables:
(a) the relation between the masses M_W and M_Z,
(b) the cross section and forward-backward asymmetry in $e^+e^- \to \mu^+\mu^-$.
To be concrete, we select two different renormalization schemes ($RS1$ and $RS2$), perform systematically the renormalization procedure, and compare the (a) and (b) results obtained in both schemes for the same set of physical input data.
These schemes are characterized as follows:

RS1: The free parameters are chosen as e, G_F, M_Z, M_H, $\{m_f\}$. The renormalization conditions are the on-shell conditions for M_Z, M_H, $\{m_f\}$, but not for M_W. Instead, the W boson self energy is renormalized at zero momentum transfer such that τ_μ is determined by G_F in the same way as in the Fermi theory. M_Z will be measured in near future with a precision of at least 0.1 GeV at LEP/SLC [15]. Together with e and G_F, this scheme directly contains those quantities which are known with best precision as free parameters. The physical W mass M_W is predicted by the pole (real part) of the renormalized W propagator. Since this scheme is a mixture of the types (i) and (ii) we shall also call it the "intermediate scheme".

RS2: This is the on-shell scheme with the free parameters e, M_W, M_Z, M_H, $\{m_f\}$. Now the on-shell condition is also imposed on the W self energy. The numerical value for M_W can be calculated from the input parameters by inverting $\tau_\mu(e, M_W, M_Z, M_H, \{m_f\})$ in one-loop order. For the details we refer to [16].

Although both schemes use the same physical input, the mixing angle as well as the neutral current couplings are different in lowest order. This reflects

the fact that the separation of S matrix elements into Born terms and radiative corrections is not free of ambiguities. By studying one-loop corrections in either of the schemes, we can get an insight to which extent these contributions compensate the lowest-order differences between both schemes. This will be of special interest in cases where the lowest-order differences become large, for example in the $e^+e^- \to \bar{f}f$ forward-backward asymmetry near the Z resonance. We restrict ourselves to the simplest process $e^+e^- \to \mu^+\mu^-$ in order to exclude uncertainties e.g. due to quark fragmentation.
The result of our investigation is that in the critical region around the Z resonance the $RS1$ and $RS2$ forward-backward asymmetries are sizable different also after inclusion of one-loop corrections.

In sect. 2 of this paper the renormalization conditions defining both schemes are collated. Sect. 3 summarizes essential features of the one-loop Green functions, and sect. 4 contains the comparison of the $M_W - M_Z$ correlation. The integrated cross sections and forward-backward asymmetries calculated in $RS1$ and $RS2$ are discussed in sect. 5.

2. The schemes

Both schemes are identical with respect to the generation of counterterms yielding finite Green functions. The input parameters e, M_Z, M_H, $\{m_f\}$ are used as free physical parameters in either of the schemes. We list the renormalization conditions as follows[1]:

- The electric charge $e = \sqrt{4\pi\alpha}$ is defined by the nonrelativistic Thomson limit of the Compton scattering.

$$\hat{\Gamma}^{\gamma ee}_\mu(k^2 = 0; \not{p} = \not{q} = m_e) = ie\gamma_\mu \tag{2.1}$$

- In the limit $k^2 \to 0$ the photon-Z-mixing energy has to vanish, i.e. on-shell photons couple to fermions as in pure QED.

$$Re\ \hat{\Sigma}^{\gamma Z}_T(0) = 0 \tag{2.2}$$

- The residue of the photon propagator is 1:

$$\frac{1}{k^2}\ Re\ \hat{\Sigma}^{\gamma}_T(k^2)\Big|_{k^2=0} = 0 \tag{2.3}$$

[1] $\hat{\Sigma}$, $\hat{\Gamma}$ denote renormalized self energies and vertices.

- The physical masses given as the poles of the propagators are equal to their lowest order values by fixing the mass counterterms δM_Z^2, δM_H^2, $\{\delta m_f^2\}$ according to

$$Re\ \hat{\Sigma}_T^Z(M_Z^2) = 0 \quad , \quad Re\ \hat{\Sigma}^\eta(M_H^2) = 0 \quad , \quad Re\ \hat{\Sigma}^f(m_f^2) = 0 \tag{2.4}$$

- To determine the wave function renormalization constants, we take into account additional residue conditions:

$$\frac{1}{\not{p} - m_{i-}} Re\ \hat{\Sigma}^{i-}(p)\Big|_{\not{p}=m_{i-}} = 0 \tag{2.5}$$

$$\frac{\partial}{\partial p^2} Re\ \hat{\Sigma}^\eta(p^2)\Big|_{p^2=M_H^2} = 0 \tag{2.6}$$

$i-$ means the $I_3 = -1/2$ component of the fermion doublet i. In both schemes we have only one renormalization constant for each field multiplet and therefore we are not able to demand a propagator residue 1 for all particles.

The next renormalization condition distinguishes between the two schemes:

(i) *Intermediate scheme*: This scheme uses the Fermi constant G_F that is related to the muon lifetime τ_μ as physical parameter. The numerical value of τ_μ is one of the input data and experimentally measured with high precision. It is calculated by considering all electroweak corrections to muon decay. The result can be split into a "weak" four-fermion interaction part with coupling G_F and, on the other side, its electromagnetic corrections which are ultraviolet convergent and gauge invariant. In particular one has up to the first order in the expansion parameter α [17]

$$\tau_\mu^{-1} = G_F^2 \frac{m_\mu^5}{192\pi^3} \left(1 - 8\frac{m_e^2}{m_\mu^2}\right) \left[1 + \frac{\alpha}{2\pi}(\frac{25}{4} - \pi^2)\right] \tag{2.7}$$

and G_F comes out at

$$G_F = 1.16634 \pm 0.00002\ 10^{-5} GeV^{-2}$$

Taking this condition one gets the relation

$$\frac{G_F}{\sqrt{2}} = \frac{g_2^2}{8M^2}$$

which can be expressed in free parameters as

$$M^2 = \frac{1}{2}M_Z^2 \left[1 + \left(1 - \frac{e^2}{\sqrt{2}G_F M_Z^2}\right)^{1/2}\right] \tag{2.8}$$

M is an abbreviation and approximates the mass M_W of the charged vector bosons $W^\pm$ in lowest order:

$$M_W = M + \sum_{n=1}^{\infty} M_n \alpha^n \tag{2.9}$$

Equation (2.7) also supplies us with a 1-loop renormalization condition containing the renormalized W self energy and the renormalization constants δZ_1^W, δZ_2^W for the SU(2) coupling g_2 and the gauge field triplet:

$$Re\left\{\frac{\hat{\Sigma}_T^W(0)}{M^2} + \frac{\alpha}{4\pi}\left(\frac{6}{\sin^2\theta} + \frac{7 - 4\sin^2\theta}{2\sin^4\theta}\ln\frac{M^2}{M_Z^2}\right) + \right.$$
$$\left. + \ 2(\delta Z_1^W - \delta Z_2^W) + \frac{\alpha}{4\pi}\frac{4}{\sin^2\theta}\left(\frac{2}{\epsilon} - \ln\gamma - \ln\frac{M^2}{4\pi\mu^2}\right)\right\} = 0 \tag{2.10}$$

To lowest order the weak mixing angle θ diagonalizing the γZ mass matrix is given by

$$\cos\theta = \frac{M}{M_Z} \tag{2.11}$$

(ii) *On-shell scheme*: In this scheme the charged vector bosons $W^\pm$ are renormalized on their mass shells. By means of the renormalization condition

$$Re\ \hat{\Sigma}_T^W(M_W^2) = 0 \tag{2.12}$$

the physical mass M_W is incorporated into the scheme as a free and renormalized parameter. It is an essential attribute of the on-shell scheme that it treats the neutral and charged vector bosons identically. We define the Weinberg angle θ_W by the mass ratio

$$\cos\theta_W = \frac{M_W}{M_Z} \tag{2.13}$$

Note that the Weinberg angle θ_W is introduced for convenience only. It is not an independent parameter in either of the schemes.

As far as the renormalization of the "unphysical" (longitudinal gauge boson, unphysical Higgs, ghost) self energies is concerned, the above list of conditions is not complete. For our purpose of calculating radiative corrections to scattering processes between light fermions ($m_f^2 \ll M_W^2$), however, it is sufficient to deal within the framework defined above. We have passed through the complete program but do not give the somewhat lengthy details at this place [**12,18**].

3. Comparison of Green functions

Differences between Green functions calculated in both schemes can be traced back to two sources:
(a) The values of parameters like W mass, mixing angle, or neutral couplings are different in both schemes.
(b) The counterterms depend in their finite parts on the renormalization conditions.
The imaginary parts of one-loop self energy- and vertex-functions are finite by themselves and consequently do not give any information about point (b). Therefore we shall discuss only real parts here. For the vector boson self energies, it is convenient to introduce the relative quantities

$$\Pi^{\gamma} = \frac{Re\ \hat{\Sigma}_T^{\gamma}(k^2)}{k^2} \quad , \quad \Pi^{\gamma Z} = \frac{Re\ \hat{\Sigma}_T^{\gamma Z}(k^2)}{k^2}$$
$$\Pi^{W} = \frac{Re\ \hat{\Sigma}_T^{W}(k^2)}{k^2 - M_{(W)}^2} \quad , \quad \Pi^{Z} = \frac{Re\ \hat{\Sigma}_T^{Z}(k^2)}{k^2 - M_Z^2} \tag{3.1}$$

The main results can be summarized as follows:

- The photon self energies of the two schemes are nearly identical except of their different thresholds $k^2 = 4M^2$ resp. $k^2 = 4M_W^2$ corresponding to the process $\gamma \to W^+W^-$.
- The W-boson self energy corrections Π^W in the intermediate scheme are generally smaller than those in the on-shell scheme, with the exception of the region around the pole $k^2 = M^2$, in which Π_{RS1}^W is ill defined because of non vanishing radiative corrections $Re\ \hat{\Sigma}_T^W(M^2) \neq 0$. For PETRA energies ($40\ GeV$) we have ($M_Z = 93\ GeV$)

$$\Pi_{RS1}^W \simeq \begin{cases} -0.006 & ; M_H = 10\ GeV \\ -0.007 & ; M_H = 300\ GeV \end{cases}$$

$$\Pi_{RS2}^W \simeq \begin{cases} -0.070 & ; M_H = 10\ GeV \\ -0.078 & ; M_H = 300\ GeV \end{cases}$$

- The counterterms contributing to $Re\ \hat{\Sigma}_T^Z(k^2)$ are proportional to $(k^2 - M_Z^2)$ in both schemes. Thus Π_{RS1}^Z differs from Π_{RS2}^Z mainly by a different renormalization constant δZ_2^Z. If we chose $M_Z = 93\ GeV$, we obtain

$$\Pi_{RS1}^Z - \Pi_{RS2}^Z \approx 0.07 \ - \ 0.08$$

In particular for PETRA energies:

$$\Pi_{RS1}^Z \simeq \begin{cases} +0.003 & ; M_H = 10\ GeV \\ +0.004 & ; M_H = 300\ GeV \end{cases}$$
$$\Pi_{RS2}^Z \simeq \begin{cases} -0.068 & ; M_H = 10\ GeV \\ -0.075 & ; M_H = 300\ GeV \end{cases}$$

- In a similar way, the mixing energy corrections $\Pi_{RS1}^{\gamma Z}$ and $\Pi_{RS2}^{\gamma Z}$ are mainly distinguished by a constant around -0.05 . But now the one-loop corrections are larger in the intermediate scheme. For example, in the PETRA region:

$$\Pi_{RS1}^{\gamma Z} \simeq \begin{cases} -0.052 & ; M_H = 10\ GeV \\ -0.055 & ; M_H = 300\ GeV \end{cases}$$
$$\Pi_{RS2}^{\gamma Z} \simeq \begin{cases} -0.003 & ; M_H = 10\ GeV \\ -2\ 10^{-4} & ; M_H = 300\ GeV \end{cases}$$

Consider the neutral couplings

$$v_f = \frac{I_3^f - 2Q^f \sin^2\theta}{2 \sin\theta \cos\theta} \quad , \quad a_f = \frac{I_3^f}{2 \sin\theta \cos\theta} \tag{3.2}$$

of the Z-boson to fermions f. In case of $I_3 = -1/2$ leptons, the numerator of v_f is small and very sensitive to $\sin^2\theta$. As a consequence, the difference between the mixing angles $\sin^2\theta$ and $\sin^2\theta_W$ is sufficient to make $(v_e)_{RS1}$ nearly twice as large as $(v_e)_{RS2}$. The axial vector couplings a_f are not very different in both schemes. The differences in the vector couplings are essentially removed by the γZ mixing energy, whereas the Z self energy leaves the ratio v_f/a_f unchanged.

- Differences between the real one-loop parts of the renormalized gauge-boson fermion vertex functions calculated in our two schemes are smaller than 10^{-3} in the range $|k^2| \leq (150\ GeV)^2$ and are therefore of minor importance.

4. Prediction of the W-mass

From either of the schemes we obtain a prediction of the W-mass in terms of all other particle masses, the fine structure constant α and the muon lifetime.

(i) *Intermediate scheme*: Consider the transverse part of the two-point (one-particle irreducible) Green function

$$\Gamma_T^W(k^2) = k^2 - M^2 + \hat{\Sigma}_T^W(k^2) \tag{4.1}$$

The mass M_W of the charged vector bosons is determined by the zero of Γ_T^W. This means that the propagator $[\Gamma_T^W(k^2)]^{-1}$ has a pole at the physical mass $k^2 = M_W^2$ required by the interpretation of the theory in terms of particles. It should be emphasized that the zero of equation (4.1) depends on the order of the radiative corrections collected in $\hat{\Sigma}_T^W$. If we substitute (2.9) into equation (4.1) and take into account only parts up to the first order in α, we will find

$$M_W = M + \alpha M_1 \tag{4.2}$$

with

$$\alpha M_1 = -\frac{1}{2M} Re\ \hat{\Sigma}_T^W(M^2)$$

The results given by this formula are very close to those determined numerically from (4.1).

(ii) *On-shell scheme*: The renormalization condition (2.12) ensures that the parameter M_W has the meaning of the charged vector boson mass. It is related to α and the other masses via the μ^- lifetime τ_μ in one-loop order [**16**]:

$$\frac{1}{\tau_\mu} = \frac{\alpha^2}{384\pi} \frac{m_\mu^5}{(M_W \sin\theta_W)^4} \left(1 - 8\frac{m_e^2}{m_\mu^2}\right) \left\{1 + 2\,\frac{\hat{\Sigma}_T^W(0)}{M_W^2} + \right.$$
$$\left. + \frac{\alpha}{2\pi} \frac{1}{\sin^2\theta_W} \left[6 + \frac{7 - 4\sin^2\theta_W}{2\sin^2\theta_W} \ln\frac{M_W^2}{M_Z^2}\right] + \frac{\alpha}{2\pi}\left(\frac{25}{4} - \pi^2\right)\right\} \tag{4.3}$$

Replacing τ_μ by G_F with help of (2.7), we are able to evaluate M_W numerically from (4.3) and (2.13) as a function of the given input parameters e, G_F, M_Z, M_H, and $\{m_f\}$.

Table 1 shows the W-masses which will be predicted by the two renormalization schemes via (4.1) resp. (4.3) for a given Z and Higgs mass. The other masses are the same as in [**16**]. The deviations of both schemes amount between 10 and 50 MeV. Thus they are much smaller than those due to variation of Higgs mass within each scheme. For the present experimental average of $M_Z = 93.0\ GeV$ the difference is even smaller than 10 MeV if $M_H \leq 300\ GeV$.

5. Comparison of cross sections and forward-backward asymmetries

We have calculated the virtual 1-loop corrections to the e^+e^- annihilation into muon pairs in both the intermediate and the on-shell scheme. To remove the infrared problem occured, bremsstrahlungs diagrams have been taken into account. The resulting *inclusive* cross section is free of infrared divergencies, but it depends on an energy cut $\Delta E/E$ and/or acollinearity cuts. We have used the soft photon approximation [**19**] and therefore $\Delta E/E = 0.1$ will be reasonable. Beside the parameters used in [**16**], we have chosen the masses

$$M_Z = 93\ GeV \quad , \quad M_H = 100\ GeV$$

which imply the mixing angles and neutral current couplings given in Table 2. We shall discuss the renormalization scheme dependence of the cross section in three points:

(i) *PETRA energies*: The differential cross sections calculated in RS1 and RS2 are in excellent agreement for center of mass energies $\sqrt{s}$ lower than 60 GeV. Electromagnetic contributions depend crucially on the experimental cuts. For our $\Delta E/E$, they are the dominant corrections to the Born approximation. Within small deviations, they are the same in both schemes. The weak corrections to $(d\sigma/d\Omega)_{RS1}$ are vanishingly small. In the on-shell scheme, however, the Born term $\propto a_e^2$ is enhanced by the Z boson energy

$$\frac{\alpha^2}{4s} a_e^2\ 2\cos\Theta\ \frac{s}{s - M_Z^2}(1 - Re\ \Pi^Z)\Big|_{RS2} \simeq$$
$$\frac{\alpha^2}{4s}\ 2\cos\Theta\ Re \frac{s}{s - m_Z^2 + \hat{\Sigma}_T^Z(s)}\Big|_{RS2}$$

with Π^Z from (3.1). This is numerically very close to

$$\frac{\alpha^2}{4s} a_e^2 \, 2\cos\Theta \, \frac{s}{s - M_Z^2}\bigg|_{RS1}$$

Table 3 shows the forward-backward asymmetry

$$A_{FB}(x) \equiv \frac{\displaystyle\int_0^x d\cos\Theta \left(\frac{d\sigma}{d\Omega}\right) - \int_{-x}^0 d\cos\Theta \left(\frac{d\sigma}{d\Omega}\right)}{\displaystyle\int_0^x d\cos\Theta \left(\frac{d\sigma}{d\Omega}\right) + \int_{-x}^0 d\cos\Theta \left(\frac{d\sigma}{d\Omega}\right)} \tag{5.1}$$

and the contributions of the various corrections (x=1, $\sqrt{s} = 34.5\ GeV$).

(ii) *Integrated cross section*: In the energy range 40 $GeV < \sqrt{s} < 140\ GeV$ the integrated cross sections of $RS1$ and $RS2$, although different in lowest order, agree well after including weak and electromagnetic corrections. This holds especially on resonance $\sqrt{s} = M_Z$, where the difference $\sigma^{RS1} - \sigma^{RS2}$ is smaller than 1 pb.

(iii) *Forward-backward asymmetry*: The two forward-backward asymmetries A_{FB}^{RS1} and A_{FB}^{RS2} are plotted as functions of the center of mass energy $\sqrt{s}$ in Figure 1 (lowest order) and in Figure 2 (including 1-loop and bremsstrahlungs corrections). Obviously the agreement between both schemes is good outside the resonance region. Therefore we shall restrict ourselves to discuss only the resonance region, in particular the interval I: $|\sqrt{s} - M_Z| < 10\ GeV$. In lowest order, A_{FB} can approximately be divided into two components:[1]

$$A_{FB}^{Born}(x) = \frac{x}{1+\frac{1}{3}x^2} \, \frac{2a^2 Re(\chi_0) + 4v^2a^2|\chi_0|^2}{1 + 2v^2 Re(\chi_0) + (v^2+a^2)^2|\chi_0|^2}$$

$$\to A_{FB}^{Born}(x)\Big|_I \simeq \frac{x}{1+\frac{1}{3}x^2}\Big\{\frac{2a^2}{1+(v^2+a^2)^2|\chi_0|^2} \, Re(\chi_0) + \frac{4v^2a^2}{1+(v^2+a^2)^2|\chi_0|^2} \, |\chi_0|^2\Big\} \tag{5.2}$$

[1] The reduced propagators χ_0 are defined as

$$\chi_0(s) = \frac{s}{s - M_Z^2 + iM_Z\Gamma_Z}$$

with the total widths $\Gamma_Z = 2.825\ GeV$ for $RS1$ and $\Gamma_Z = 2.563\ GeV$ for $RS2$.

Their contributions to the difference of the asymmetries given in both schemes have the same sign below $\sqrt{s} = M_Z$ but opposite signs above. It turns out that the deviation of the $RS1$ and $RS2$ curves shown in Figure 1 vanishes at the upper bound of I and rises smoothly up to maximum value as $\sqrt{s}$ approaches the lower bound.
The main effects of the weak radiative corrections may be understood in terms of the following formula

$$A_{FB}^{Born+weak}\Big|_I \simeq \frac{x}{1+\frac{1}{3}x^2} \times \times \frac{2a^2 \ Re(\chi) + 4v^2a^2(1 - \frac{2}{v} Re\ \Pi^{\gamma Z})|\chi|^2}{1 + (v^2+a^2)^2(1 - \frac{4v}{v^2+a^2} Re\ \Pi^{\gamma Z})|\chi|^2} \tag{5.3}$$

in which the Z self energy is absorbed by correcting χ_0 to

$$\chi(s) = \frac{s}{s - M_Z^2 + \widehat{\Sigma}_T^Z(s)}$$

The dominating contribution to the antisymmetric $Re(\chi)$ part comes from the Z self energy, while it is the γZ mixing that governs the symmetric $|\chi|^2$ part. Having in mind our comparison of Green functions, the on-resonance asymmetry gets large corrections from the γZ mixing part in the intermediate scheme, whereas in the on-shell scheme the corrections to $A_{FB}(M_Z^2)$ are small. Because of its magnitude, the γZ mixing energy, although yielding

$$v_e^{RS1} \to v_e^{RS1}\Big[1 - \frac{1}{v_e}\,\Pi_{RS1}^{\gamma Z}(M_Z^2)\Big] \simeq v_e^{RS2} \quad ,$$

is not able to correct the *powers* of the neutral vector coupling v_e^{RS1} in (5.3) as good as expected. The seperate corrections of the on-resonance asymmetry are listed in Table 4.
The big difference between the lowest order asymmetries A_{FB}^{RS1} and A_{FB}^{RS2} is diminished by inclusion of the weak one-loop corrections, but still a non-negligible difference survives. Taking into account also two-loop contributions to $Im\ \Sigma^Z$, the results are changed only very slightly (< 0.01%). The separation between the A_{FB} values becomes even larger if the QED corrections are included:

- The Born resonance term $4v_e^2a_e^2\ 2\cos\Theta\ |\chi|^2$ in the forward-backward asymmetry is proportional to the lowest order vector coupling v_e^2, which gets very different values in both schemes. Thus the QED asymmetry corrections of order α^3 will show a clear renormalization scheme dependence.
- Furthermore, the QED contributions also decrease the integrated cross section in the denominator of (5.1). All weak corrections to A_{FB}^{Born} will be increased by an amount involved in the value of the QED correction in Table 4.

The size of our given value for the QED corrections was derived from the specific choice of $\Delta E/E = 0.1$. For realistic experimental situations, however, other cuts needing also the complete hard bremsstrahlung part may be more appropiate. The quantitative results of such QED corrections will in general be different from our values. However, the qualitative result that they are influenced by the elektroweak renormalization scheme should show up also in other experimental situations.

In conclusion, we have investigated the renormalization scheme dependence of one-loop electroweak corrections by means of two different schemes explicitly specified. We have found that the relation between M_W and M_Z is practically the same in both schemes. Also the integrated cross section and the forward-backward asymmetry for $e^+e^- \to \mu^+\mu^-$ at PETRA energies are quantities which essentially do not depend on the choice of a specific scheme. For the forward-backward asymmetry around the Z, in particular the on-resonance asymmetry, however, strikingly different predictions are obtained according to the underlying renormalization scheme. In the intermediate scheme $RS1$ the Born value of $A_{FB}(M_Z^2)$ is so much larger than in $RS2$ that this difference is not succesfully removed by inclusion of the one-loop corrections. In order to get a finally satisfactory answer about the correct A_{FB} value, next order calculations will become necessary.

References

[1] S.L. Glashow: Nucl. Phys. **22** (1961) 579;
S. Weinberg: Phys. Rev. Lett. **19** (1967) 1264;
A. Salam: in *Elementary Particle Physics*, ed. N. Svartholm (Almquist and Wiksell, Stockholm 1968) p. 367

[2] UA1 Collaboration, G. Arnison et al., Phys Lett. **126** B (1983) 398;
UA2 Collaboration, P. Bagnaia et al., Phys. Lett. **129** B (1983) 130;
UA1 Collaboration, G. Arnison et al., CERN-EP/83-162 (1983)

[3] G. 't Hooft: Nucl. Phys. B **33** (1971) 173;
Nucl. Phys. B **35** (1971) 165

[4] D.A. Ross, J.C. Taylor: Nucl. Phys. B **51** (1973) 125;
Nucl. Phys. B **58** (1973) 643(E);
S. Sakakibara: Phys. Rev. D **24** (1981) 1149;
E.A. Paschos, M. Wirbel: Nucl. Phys. B **194** (1982) 189

[5] K.I. Aoki, Z. Hioki, R. Kawabe, M.Konuma, T. Muta:
Suppl. Prog. Theor. Phys. 73 (1982) 1

[6] A. Sirlin: Phys. Rev. D **22** (1980) 971;
W.J. Marciano, A. Sirlin: Phys. Rev. D **22** (1980) 2695

[7] M. Green, M. Veltman: Nucl. Phys. B **169** (1980) 137;
Nucl. Phys. B **175** (1980) 547(E)

[8] F. Antonelli, M. Consoli, G. Corbo: Phys. Lett. **91** B (1980) 90;
F. Antonelli, G. Corbo, M. Consoli, O. Pellegrino:
Nucl. Phys. B **183** (1981) 195

[9] C.H. Llewellyn Smith, J.F. Wheater: Phys. Lett. **105** B (1981) 486;
J.F. Wheater, C.H. Llewellyn Smith: Nucl. Phys. B **208** (1982) 27

[10] G. Passarino, M. Veltman: Nucl. Phys. B **160** (1979) 151;
M. Consoli: Nucl. Phys. B **160** (1979) 208

[11] J. Fleischer, F. Jegerlehner: Phys. Rev. D **23** (1981) 2001;
W. Wetzel: Nucl. Phys. B **227** (1983) 1;
J. Cole: in [**14**];
M. Böhm, W. Hollik: Phys. Lett. **139**B (1984) 213;
W. Hollik: Phys. Lett. **152**B (1985) 121;

R.W. Brown, R. Decker, E.A. Paschos:
Phys. Rev. Lett. **52** (1984) 1192;
B.W. Lynn, R.G. Stuart: Nucl. Phys. B **253** (1985) 216;
M. Böhm, A. Denner, W. Hollik, R. Sommer:
Phys. Lett. **144**B (1984) 404

[12] M. Böhm, W. Hollik, H. Spiesberger: DESY 84-027

[13] S. Sakakibara: Z. Phys. C 11 (1981) 43

[14] *Workshop on Radiative Corrections in* $SU(2)_L \times U(1)$,
Miramare, Trieste, 6-8 June 1983, ed. B.W. Lynn, J.F. Wheater
(World Scientific Publishing Co Pte Ltd., Singapore 1984)

[15] M. Davier: "Proceedings of the LEP Summer Study" (CERN 79-01)

[16] M. Böhm, W. Hollik, H. Spiesberger: Z. Phys. C **27** (1985) 523

[17] R.E. Behrends, R.J. Finkelstein, A. Sirlin: Phys. Rev. **101** (1956)
866;
S.M. Berman: Phys. Rev. **112** (1958) 267;
T. Kinoshita, A. Sirlin: Phys. Rev. **113** (1959) 1652

[18] H.-J. Timme: Diplomarbeit, Univ. Hamburg (1985)

[19] M. Böhm, W. Hollik: Z. Phys. C **23** (1984) 31

M_Z [GeV]	RS	M_H [GeV] 10	100	300	1000
	1	75.812	75.737	75.675	75.593
88	2	75.787	75.715	75.654	75.575
	1	78.387	78.314	78.253	78.172
90	2	78.374	78.306	78.248	78.171
	1	80.890	80.819	80.759	80.679
92	2	80.887	80.821	80.764	80.690
	1	82.120	82.050	81.990	81.911
93	2	82.120	82.055	81.999	81.926
	1	83.338	83.268	83.208	83.130
94	2	83.340	83.276	83.221	83.148
	1	85.739	85.670	85.612	85.533
96	2	85.746	85.684	85.630	85.558
	1	88.103	88.035	87.977	87.898
98	2	88.114	88.052	87.999	87.929

Table 1 The W boson mass M_W in GeV
for given masses M_Z, M_H (RS : renormalization scheme)

	RS1	RS2
W mass parameter	$M = 83.121$	$M_W = 82.055$
mixing angle	$\sin^2\theta_0 = 0.2012$	$\sin^2\theta_W = 0.2215$
vector coupling	$v_e = -0.1219$	$v_e = -0.0686$
axial vector coupling	$a_e = -0.6237$	$a_e = -0.6059$

Table 2 Parameters belonging to the input data

	A_{FB}^{RS1} [%]	A_{FB}^{RS2} [%]
Born	−9.271	−8.645
photon self energy (without fermion loops)	+0.0005	+0.0005
Z self energy	+0.034	−0.614
γZ mixing	−0.003	$-5\ 10^{-6}$
vertex corrections	+0.013	+0.012
box diagrams	−0.012	−0.010
Born + weak	−9.238	−9.257
QED	+5.343	+5.201
full	−3.895	−4.056

Table 3 The forward-backward asymmetry A_{FB} for $\sqrt{s} = 34.5\ GeV$ and $|\cos\Theta| \leq 1.0$. The bremsstrahlung is included with $\Delta E \leq 0.1\ E_{beam}$.

	A_{FB}^{RS1} [%]	A_{FB}^{RS2} [%]
Born	10.565	3.772
photon self energy (without fermion loops)	−0.0001	$-2\ 10^{-5}$
Z self energy	±0.000	±0.000
γZ mixing	−8.140	+0.244
vertex corrections	−0.494	−0.253
box diagrams	−0.087	−0.077
Born + weak	1.846	3.685
QED	−8.563	−2.894
full	−6.717	0.791

Table 4 The forward-backward asymmetry A_{FB} for $\sqrt{s} = 93.0\ GeV$ and $|\cos\Theta| \leq 1.0$. The bremsstrahlung is included with $\Delta E \leq 0.1\ E_{beam}$.

Figure captions

Figure 1: The forward-backward asymmetry to $e^+e^- \to \mu^+\mu^-$ calculated in lowest order in the intermediate scheme (RS1) and the on-shell scheme (RS2).

Figure 2: The forward-backward asymmetry with full electroweak one-loop corrections in the schemes RS1 (———) and RS2 (– – – –). The photonic corrections belong to $\Delta E/E = 0.1$. "RS2(Born)" is the on-shell scheme asymmetry in Born approximation, known from Figure 1 and serving us as a reference curve (·····).

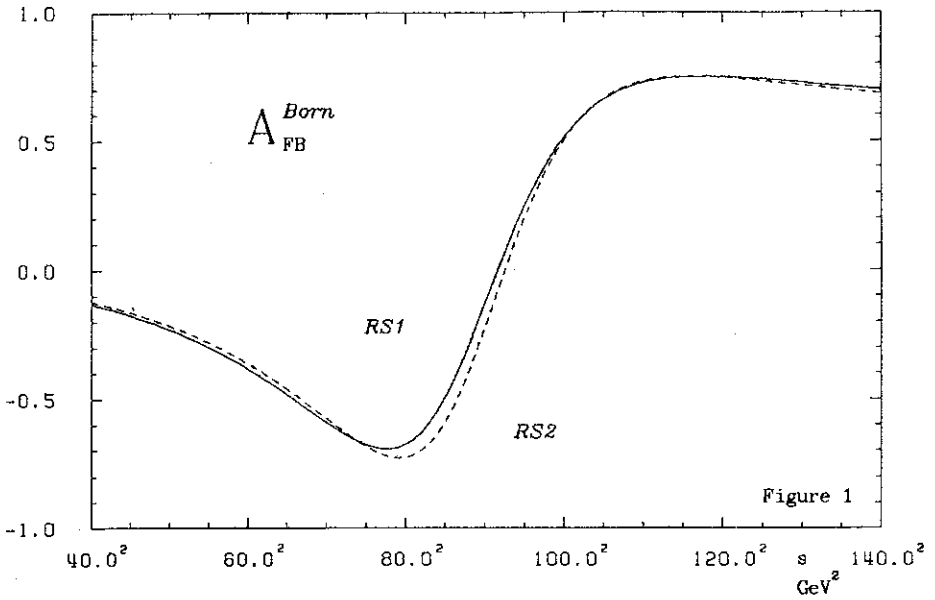
1.0
0.5
0.0
-0.5
-1.0
A_{FB}^{Born}
RS1
RS2
Figure 1
40.0^2
60.0^2
80.0^2
100.0^2
120.0^2
s
140.0^2
GeV^2

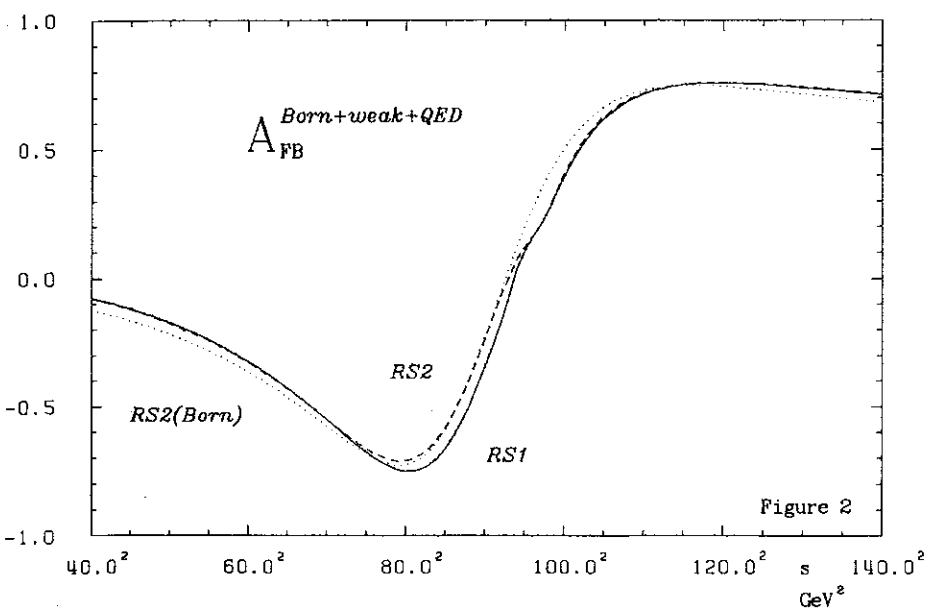
1.0
0.5
0.0
-0.5
-1.0
$A_{FB}^{Born+weak+QED}$
RS2
RS2(Born)
RS1
Figure 2
40.0^2
60.0^2
80.0^2
100.0^2
120.0^2
s
140.0^2
GeV^2